

# Local Rates of Mass Transfer from Spheres in Ordered Arrays

JOHN M. RHODES and FRED N. PEEBLES

University of Tennessee, Knoxville, Tennessee

The local mass transfer rates from a sphere in a regular packing array have been determined by measuring the local radius change of a slightly soluble 1.500-in. diameter benzoic acid test sphere after having been immersed in a water stream. Results in the form of typical local Sherwood number profiles are reported for single spheres over a particle Reynolds number range of 166 to 1,560, and for spheres in simple cubic packing and rhombohedral packing over particle Reynolds number ranges of 488 to 2,409 and 1,680 to 3,410, respectively. All runs were made at room temperature. An idealized flow pattern around spheres in simple cubic packing is presented.

Although extensive work has been done on various overall transport phenomena, such as the overall mass and heat transport from randomly packed beds to flowing fluids (1, 6, 9, 10, 12, 16, 18, 20) and from single particles such as single spheres (8, 10) or cylinders to flowing fluids, only limited references to previous investigations of the local transport phenomena from spheres in packed beds to flowing fluids are known. It was the objective of this work to investigate the local rates of mass transfer from slightly soluble spheres in a packed bed to a flowing fluid. By application of an appropriate analogy between heat and mass transfer and the local heat and mass transfer, the local heat transfer characteristics in a packed bed of spheres can be predicted from corresponding local mass transfer characteristics that can be more readily investigated in the laboratory. The present work was limited to investigation of two ordered arrays of spheres, the simple cubic packing having a void fraction of 0.47 and the rhombohedral packing having a void fraction of 0.26. These two arrays are the limiting packings expected in a bed of randomly packed spheres that has an average void fraction of 0.38 to 0.40.

## THEORY

In the investigation of the local rates of mass transfer from slightly soluble spheres in a packed bed molecular diffusion, natural convection mass transfer and forced convection mass transfer may be of importance at a given location on a sphere. Of course, with a fluid flowing through the packed bed, it would be expected that the primary mechanism of mass transfer would be by forced convection. However, in regions on a sphere adjacent to a point of contact between spheres, the theory of real fluids indicates that fluid velocities are very low. Hence, one would expect that mass transfer would be due primarily to the mechanisms of molecular diffusion and natural convection in these regions. Since the mass transfer coefficients for molecular diffusion are orders of magnitude less than those for forced convection, one would expect a large variation in the local mass transfer rates from a slightly soluble sphere in a packed bed. It is this variation of local mass transfer rates that is the subject of this investigation.

For the present case of a slightly soluble sphere, the time-average rate of mass transfer from the sphere surface to the flowing stream could be determined on an overall basis from the weight loss of the sphere. It follows that the local rate of mass transfer from the sphere would be related to the local radius change. For small changes of

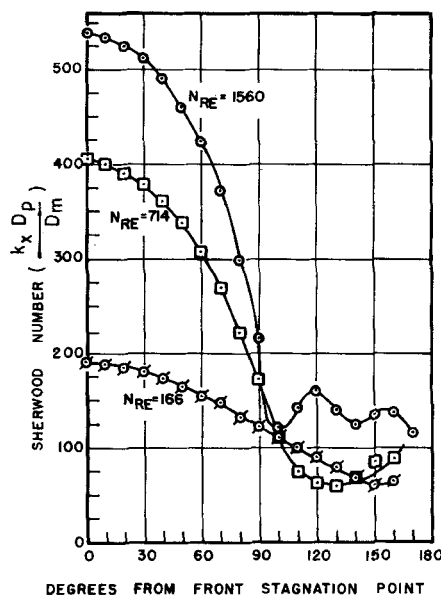


Fig. 1. Single sphere results. Local Sherwood number vs. position on sphere.

radius, that is, small  $\Delta r/r$  ratios, the assumption that a local  $\Delta r$  varies linearly with time can be made. One can then equate the expression for the rate of mass transfer by diffusion in liquids that is developed in a number of texts on mass transfer fundamentals (2, 19, 30) to the expression for mass loss from the sphere as follows

$$N_A = k_s \Delta X = \frac{\rho_{BA} \Delta r}{M_{BA} \Delta t} \quad (1)$$

That is, by measuring the local radius change in a period  $\Delta t$  and knowing the concentration gradient involved, one can calculate the local mass transfer coefficient.

In this work, as the bulk fluid had a negligible concentration of the dissolving solute, the concentration gradient simply had the value of the mole fraction of benzoic acid in a saturated water solution.

The mass transfer coefficient can be expressed in terms of the dimensionless group  $k_s D_p M_w / \rho_w D_v$ , which has been termed the Sherwood number.

$$N_{SN} = \frac{\rho_{BA} M_w D_p \Delta r}{\rho_w M_{BA} D_v X_{sat} \Delta t} \quad (2)$$

TABLE 1.

Run	Packing	$N_{Re}$	$N_{Sc}$	$\bar{N}_{Sh}$	$T, ^\circ\text{C.}$	$D_v, \text{cm.}^2/\text{sec.}$	$X_{sat}$
59-5	single sphere	166	900	122	27.9	$0.930 \times 10^{-5}$	$5.63 \times 10^{-4}$
71-1	single sphere	461	890	210	28.1	0.936	5.67
58-4	single sphere	714	917	194	27.5	0.921	5.55
60-6	single sphere	990	935	261	27.1	0.912	5.48
61-7	single sphere	1,260	944	258	26.9	0.907	5.44
63-8	single sphere	1,560	908	274	27.7	0.926	5.59
68-6	simple cubic	488	981	$\sim 510$	26.1	0.889	5.30
69-9	simple cubic	1,310	1,080	$\sim 820$	24.2	0.846	4.97
69-8	simple cubic	2,409	921	$\sim 1,000$	27.4	0.919	5.53
70-3	rhombohedral	1,680	1,120	—	23.5	0.831	4.85
70-2	rhombohedral	1,810	954	—	26.7	0.903	5.40
71-4	rhombohedral	3,410	953	—	26.7	0.903	5.40

It should be mentioned that one is justified in substituting for the density and molecular weight of the saturated solution the corresponding values for water, as was done in Equation (2). This can be done since the benzoic acid concentration is extremely low, even at saturation ( $X_{sat}$  being on the order of  $5 \times 10^{-4}$  moles BA/mole solution).

By measuring the local radius change,  $\Delta r$ , in a period  $\Delta t$ , and determining  $D_v$  and  $X_{sat}$  as functions of run temperature from the literature, the local Sherwood number can be determined from Equation (2).

For this work the volumetric diffusivity,  $D_v$ , was calculated from a general empirical correlation proposed by Wilke (23). For the benzoic acid-water system the Wilke correlation is

$$D_v = \frac{10^{-7} T}{3.85 \mu_w} \quad (3)$$

The saturated mole fraction,  $X_{sat}$ , was calculated from corresponding solubility values taken from a curve plotted through solubility data obtained from the literature (11, 15, 17, 22).

## EXPERIMENTAL

The system employed for the mass transfer rate measurements was water as the flowing fluid and benzoic acid as the slightly soluble sphere material. Benzoic acid spheres were prepared by pressing c.p. grade crystals into a rough cylindrical slug, and then machining to obtain spheres 1.500 in. in diameter with a diametric tolerance of  $\pm 0.002$  in. Measurements of the density of the machined spheres yielded an average density of 1.288 g./cu. cm. which compares favorably with the value 1.292 g./cu. cm. reported by Garner and Hoffman (3). A detailed description of the die used for pressing

the benzoic acid slugs and the steps of the sphere preparation is given in reference 13.

A test column of square cross section 7.5 in. on each side was used in the mass transfer experiments. The test section was installed in a closed loop (recirculating) water flow facility. Downward flow was used throughout.

A dispersing bed was located at a distance of 7 in. ahead of the packing. It was determined experimentally (13) that the velocity profile just ahead of the packing was essentially flat across the column to within 0.5 in. of the wall.

Local mass transfer rates from single spheres, from spheres in cubic array, and from spheres in rhombohedral array were investigated. For both packing arrays an orientation was selected in which one sphere directly followed another with respect to direction of flow. The simple cubic array was 5 spheres square by 7 spheres deep. The test sphere was located five layers down from the top in the center of a layer. The rhombohedral array might be visualized if one started with the  $5 \times 5 \times 7$  cubic array and translated the second and fourth vertical layers one-half diameter up and one-half diameter horizontally and then compressed the layers horizontally until contacting. The resulting array had horizontal dimensions of 5.75 in. by 7.5 in. The test sphere was located similarly to the cubic array case.

Experimental mass transfer runs were carried out by placing the test sphere in an assembled array of inert (insoluble) spheres. Water flow was established through the test column for a measured time interval. Upon termination of the exposure to water flow, the test sphere was removed from the column, dried, and then mounted in a special measuring jig for determination of the local radius profiles. A hollow 0.108-in. O.D. stainless steel shaft was permanently mounted in each test sphere. The shaft served as a means to orient the sphere in the measuring jig and served as a permanent space co-ordinate reference. When in the packed array the shaft ends were inserted into neighboring spheres and thus served to hold the test sphere in position while remaining hidden from the flowing water. The local radius measurements before and after a run were subtracted to obtain a local radius change.

Changes in radius up to 0.0300 in. were observed. Radius measurements were recorded to 0.0001 in. with an average

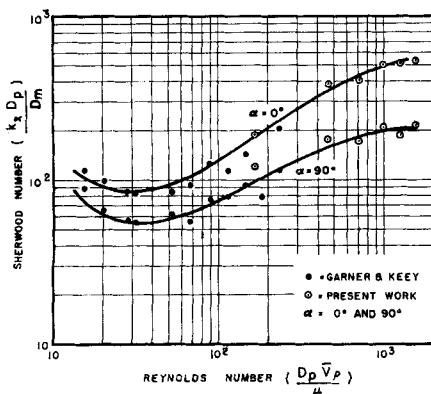


Fig. 2. Comparison of results of Garner and Key (4) and present results for local Sherwood number vs. particle Reynolds number at  $\alpha = 0$  and  $90$  deg. on the sphere.

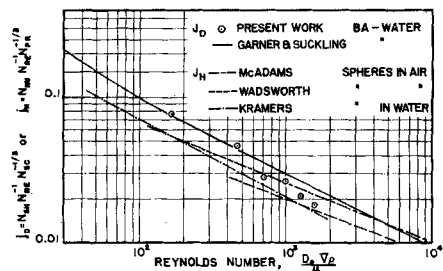


Fig. 3. Colburn  $j_D$  vs. particle Reynolds number. Comparison of overall single sphere results of present work with Wadsworth (21), Garner and Suckling (5), McAdams (9), and Kramers (7).

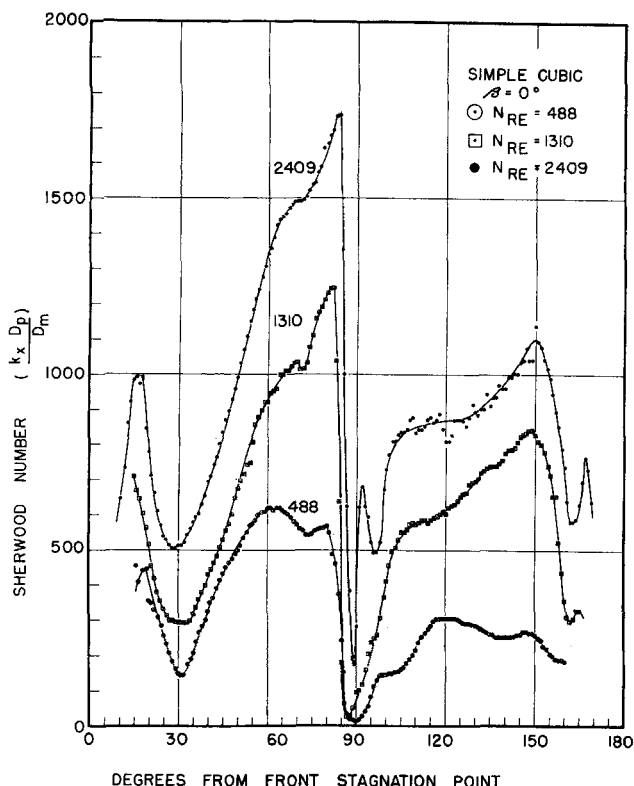


Fig. 4. Local Sherwood number profiles for spheres in simple cubic packing. Profile position angle:  $\beta = 0$  deg.

error of  $\pm 0.00015$  in. or a probable error of 0.00018 in. (14). As the calculation of radius change involved subtraction of two local radius measurements, systematic errors were assumed to be eliminated. The probable error of a radius change measurement was calculated to be 0.00025 in. Therefore, the probable percentage error varied from 0.8 to 5%, depending on the local radius change.

## EXPERIMENTAL RESULTS

### Single Sphere Results

While the chief purpose of this investigation was to determine the local mass transfer rates around spheres in packed beds, it was considered important to establish the reliability of the experimental techniques used by comparing results obtained in this work with results of other workers. For this purpose, a series of six single-sphere runs was made in which local mass transfer rates were determined over a particle Reynolds number range of 166 to 1,560. The particle Reynolds number was calculated for both single sphere and packed bed cases using the sphere diameter and the superficial velocity. Results of these runs are presented in Figure 1 as plots of the local Sherwood number versus the position on the sphere.

Run parameters and associated material properties are tabulated in Table 1 for the single sphere runs, the simple cubic packing runs, and the rhombohedral packing runs. The values for the average Sherwood number,  $\bar{N}_{sh}$ , were calculated from local Sherwood number profiles for the single sphere and simple cubic cases, but were not obtained for the rhombohedral cases.

It is known that the rate of mass transfer from a solid to a fluid by forced convection is dependent on the flow rate of the fluid. Therefore, for the single sphere it would be expected that the local rate of mass transfer could be predicted from the local velocity of the fluid. From the boundary layer theory of flow around a single sphere as discussed by Garner and Keey (4), one would expect the mass transfer rate to decrease from a maximum at the

forward stagnation point to a minimum value at a position at 108 to 110 deg. This minimum mass transfer rate would correspond to the ring of separation for the boundary layer. Behind this ring of separation in the wake region of flow around a sphere, one would expect the rate of mass transfer to increase to another maximum at the rear stagnation point. As is seen in Figure 1, the results of the present work generally follow the mass transfer profile that is expected from boundary layer theory.

**Comparison of Present Work with Local  $N_{sh}$  Data of Garner and Keey (4).** Comparisons of the local mass transfer rates obtained in the above set of runs were made with the local mass transfer rate profiles also taken from the benzoic acid-water system that were presented in the work of Garner and Keey (4). Plots of  $N_{sh}$  versus  $N_{Re}$  at two positions on a sphere are presented in Figure 2. It is evident that there is good agreement in these forward regions of the spheres.

It was observed that the separation ring shifted forward with increasing Reynolds number. This observation agrees with that reported by Garner and Keey (4) and by Wadsworth (21).

**Comparison of Overall  $N_{sh}$  from Present Work with Literature.** By a numerical integration of the local Sherwood number over the surface of a sphere, an overall Sherwood number was calculated for each run. Comparisons were made with the overall heat transfer around single spheres taken from McAdams (9), with an extrapolation of Wadsworth's correlation (21) of overall heat transfer around a single sphere, and with Kramers' (7) correlation for spheres cooled by water.\* The data are compared on a plot of Colburn  $j_D$  and  $j_H$  factors versus  $N_{Re}$  in Figure 3.

From the above comparisons between the present work and the correlations from the literature, it was concluded

\* McAdams (9) and Wadsworth (21) gave correlations of heat transfer data in the form of  $N_{Sh} = a N_{Re}^b$ . It was necessary to convert these correlations to the Colburn  $j$  factor form shown in Figure 3.

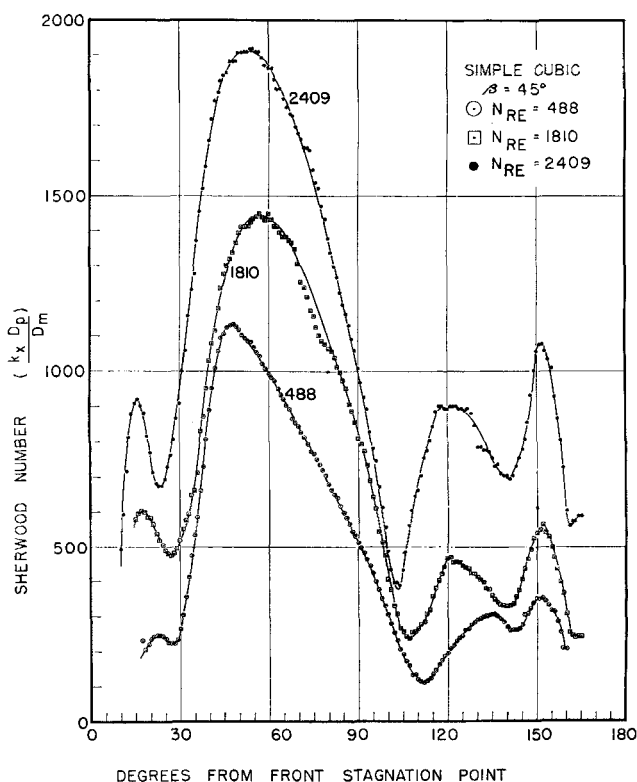


Fig. 5. Local Sherwood number profiles for spheres in simple cubic packing. Profile spheres in simple cubic packing. Profile position angle:  $\beta = 45$  deg.

that the system designed for this investigation and the techniques developed for manufacturing and measuring the test spheres were satisfactory for the continuation of the work to be packed bed investigations.

### Simple Cubic Packing Results

A series of runs was made with the test spheres in a packed bed in simple cubic array, which had a void fraction of 0.4764. Results are presented in Figures 4 and 5 for particle Reynolds numbers of 488, 1,310, and 2,409. Local mass transfer rate profiles were taken at 22.5 deg. increments around the sphere, starting with a profile through a side contact point. Because of symmetry of the packing, the profiles were reduced to three sets of profiles that have been defined at three characteristic angles:  $\beta = 0$  deg., 22.5 deg., and 45 deg.

Data for  $\beta$  angles that were equivalent due to symmetry (for example, at  $\beta = 0, 90, 180$ , and  $270$  deg., all of which were through side contact points; or at  $\beta = 5, 85, 95, 175, 185, 265, 275$ , and  $355$  deg., all of which were 5 deg. from a side contact point, etc.) were combined by averaging the  $\Delta r$  values from four such profiles point by point in angle  $\alpha$  to obtain an average profile for a given  $\beta$  angle.

**Flow Pattern around Spheres in Simple Cubic Array.** The regularity of the locations of maximum and minimum points on the profiles in Figures 4 and 5 suggested that the pattern of the fluid streamlines adjacent to the sphere in a packed bed could be inferred from the local mass transfer data. In this regard, by using the known flow pattern around a single sphere as a guide, it is suggested that the flow pattern around the sphere in simple cubic packing has the following characteristics.

1. The region around the forward contact point,  $\alpha = 0$  to  $10$  deg., is a region of minimum mass transfer rate.

While this statement has not been supported with experimental data in this paper, subsequent work by the author has provided verification over a wide range of Reynolds numbers. The reason for no data existing in these regions of forward and rear contact points is that the experimental technique required the test sphere mounting shaft to be located on this axis, thus preventing data acquisition. Mass transfer is essentially by molecular diffusion and natural convection within this region.

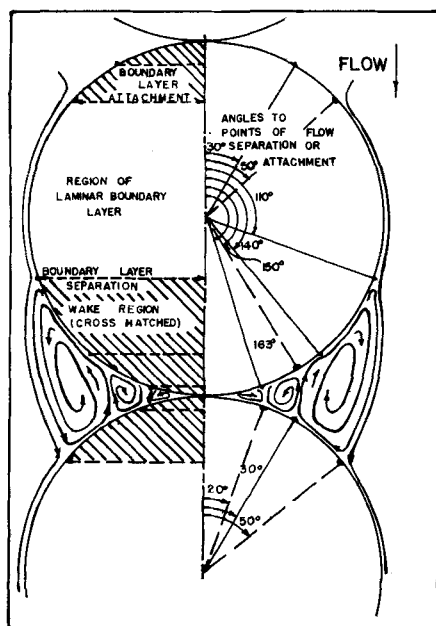


Fig. 6. Flow pattern around sphere in simple cubic array.

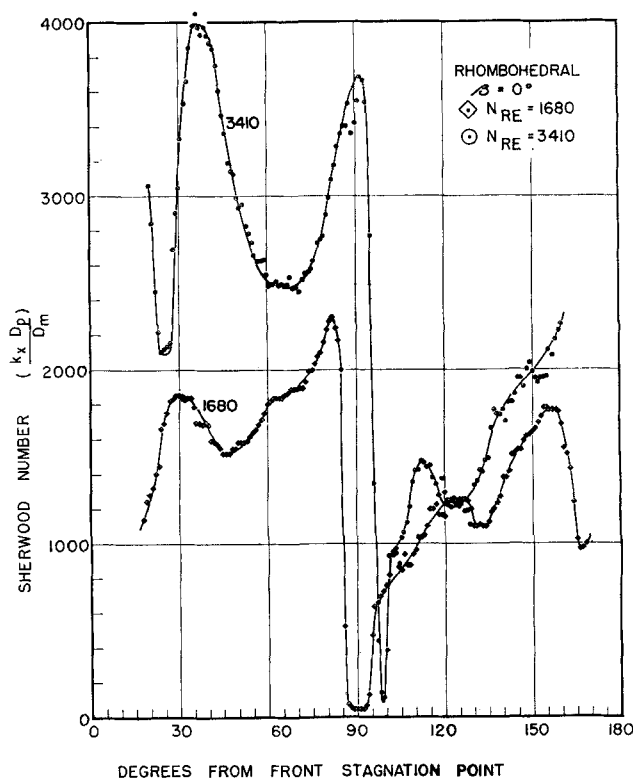


Fig. 7. Local Sherwood number profiles for spheres in rhombohedral packing. Profile position angle:  $\beta = 0$  deg.

2. Around  $\alpha = 18$  to  $20$  deg., a local maximum mass transfer rate occurs, while between  $\alpha = 25$  to  $30$  deg. a local minimum occurs. It is suggested that within the region forward of this point a minor eddy of the wake region from the preceding sphere exists. That is, eddy flow impinges on the sphere at the  $\alpha = 18$  to  $20$  deg. maximum location and divides into two streamlines: one circling upward forming a minor eddy, the other circling downward and separating at the minimum ring of transfer between  $\alpha = 25$  to  $30$  deg.

3. The overall maximum mass transfer rate occurs between  $\alpha = 50$  to  $60$  deg. It is suggested that this is the ring of attachment of boundary layer from the sphere above. At this ring of attachment, the mass transfer rates reach values as great as 2.2 to 3 times the average values for the sphere in simple cubic array, over the Reynolds number range covered in this investigation. A streamline impinging at this location splits into two streamlines: one circling upward forming the principal eddy of the wake of the preceding sphere, the other streamline attaching itself as a laminar boundary layer that follows along the sphere surface until it reaches a ring of separation, shown in Figure 5 to exist between  $\alpha = 103$  to  $122$  deg. It should be noted that this ring of separation appears to move forward with increasing Reynolds number just as observed by Garner and Keey (4), by Wadsworth (21), and as reported in the present work in the preceding section.

4. It should be noted from Figure 4 that a region of essentially zero mass transfer rate exists around  $\alpha = 90$  deg. The width of this region is approximately 8 to 10 deg. The region corresponds to a point of contact between spheres. Therefore, flow streamlines for the set of profiles in Figure 4 are distorted from those in Figure 5 because of the contact point at  $\alpha = 90$  deg.; however, it appears that the general flow pattern described above exists along these profiles, also.

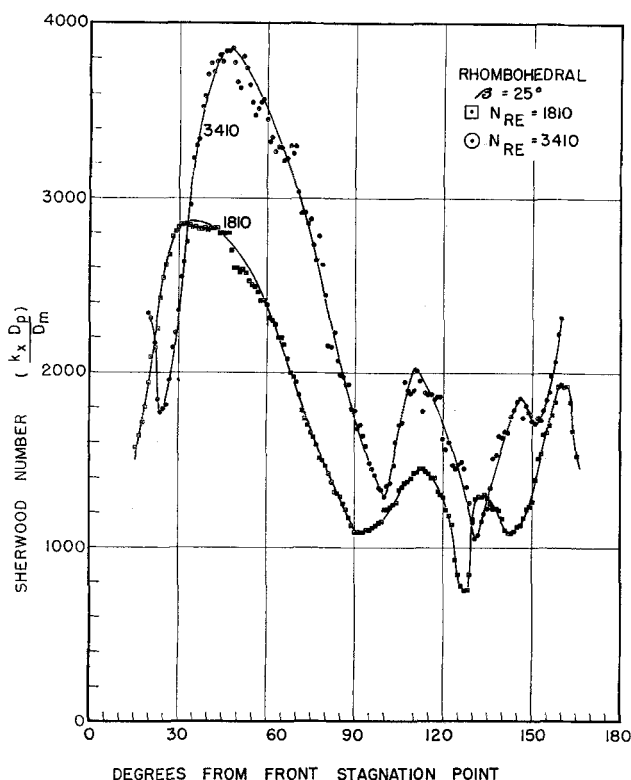


Fig. 8. Local Sherwood number profiles for spheres in rhombohedral packing. Profile position angle:  $\beta = 25$  deg.

5. The region to the rear of the separation ring for the boundary layer is a wake region similar to that for a single sphere. It contains three local maximum mass transfer rates, at  $\alpha = 120, 150$ , and  $170$  deg., with minimum mass transfer rates at  $\alpha = 140, 160$ , and  $180$  deg. This suggests that a three-eddy complex exists in the wake region. In general, the local mass transfer rates in the wake region are less than the average over the entire sphere.

Figure 6 shows the streamlines for flow past a sphere in the simple cubic array, as suggested by the mass transfer data. This sketch was made with separation locations taken from a simple cubic profile at a position of  $\beta = 45$  deg. from the side contact points. It should not be taken as being a general figure that would describe the flow pattern around the entire sphere in simple cubic array, because the locations of the separation rings vary periodically around the sphere. These variations in latitudinal position of the separation ring are caused by secondary flow fields set up around points of contact between adjacent spheres. This secondary flow distorts the streamline locations from those shown but does not radically alter the flow patterns around the sphere in simple cubic array.

**Points of Contact.** It is apparent from Figure 4 that the local mass transfer rate in the region adjacent to a point of contact between spheres is essentially zero. From observations made on spheres subjected to long runs, it was determined that the regions of minimum mass transfer rate at the forward and rear stagnation points were on the order of  $20$  deg. across, while the region at a point of contact on the side of a sphere was only about  $10$  deg. across. More definite observations in these areas cannot be drawn from the present investigation because it was necessary to limit the length of a run in order to restrict the maximum radius change to a value chosen so that the deviation of the test sphere shape from spherical shape would not significantly affect the flow pattern. Further investigation is required in the regions of contact between spheres. Perhaps by coating a test sphere with lacquer

over the surface, except in the regions of contact points, the present techniques can be used for such investigation.

Regarding further investigation of the points of contact regions, the Schmidt number is an important parameter for the mass transfer in these regions of mass transfer by molecular diffusion. Any further investigation of the mass transfer rates in these regions should include an extensive investigation of the Schmidt number effect on the size of the regions of low mass transfer rates around contact points.

#### Rhombohedral Packing Results

A series of runs was made with the test sphere in a packed bed in rhombohedral array that has a theoretical void fraction of  $0.2595$ . The orientation of the packed was such that each sphere was entirely behind another sphere in the flowing stream. This rhombohedral orientation gave the limiting case for investigating the extremes of local mass transfer rates.

Results are presented at particle Reynolds numbers of  $1680, 1810$ , and  $3410$  in Figures 7 through 10.

As in the case of simple cubic packing, the surface of a sphere in a rhombohedral array has regions of symmetry. Thus, in this case a complete pattern of flow around the sphere could be defined by investigating the local mass transfer profiles for one-fourth of the surface. Profiles were determined at a characteristic angle  $\beta = 0$  deg. (having contact at a side point and on top and bottom); at  $\beta = 25$  deg. (no contacts except at the top and bottom); at  $\beta = 54$  deg.  $45$  min. (contact points at top, bottom, and at  $\alpha = 60$  and  $120$  deg. on the side); and at  $\beta = 90$  deg. (having no contacts except at top and bottom).

**Flow Pattern around Spheres in Rhombohedral Array.** As was the case for spheres in simple cubic array, a degree of regularity between the mass transfer rate profiles is evident in Figures 7 through 10. The flow pattern appears much more complex for the rhombohedral case, however. The mass transfer profiles for spheres in rhombohedral array appear to have the following characteristics:

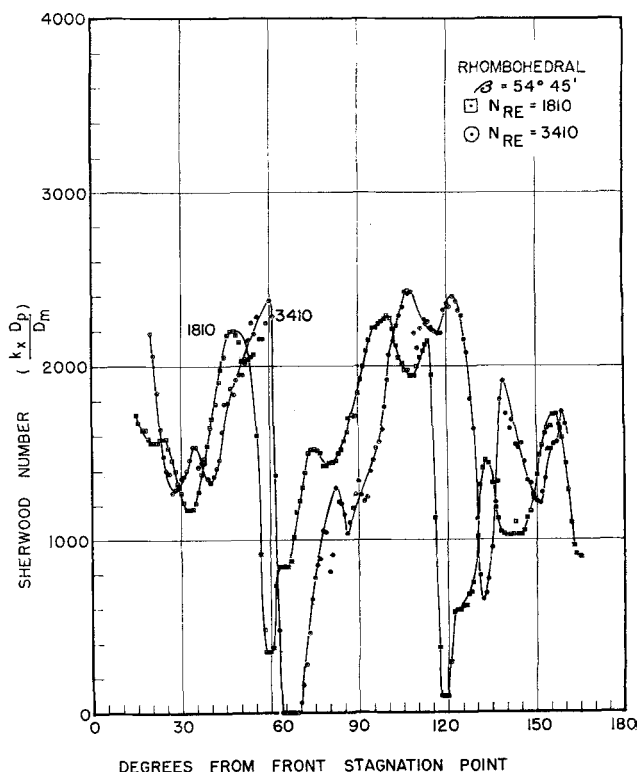


Fig. 9. Local Sherwood number profiles for spheres in rhombohedral packing. Profile position angle:  $\beta = 54$  deg.  $45$  min.

1. As for simple cubic array, a region of minimum mass transfer rates exists around the forward contact point. This region appeared to cover the surface included in a solid angle of 20 deg.

2. Figures 8 and 10, illustrating mass transfer rate profiles at position angles at  $\beta = 25$  deg. and  $\beta = 90$  deg. (that is, having no points of contact other than at top and bottom), are quite similar to Figure 5, the profile for simple cubic packing at a position angle of  $\beta = 45$  deg. to the contact points. Regions of forward wake, boundary layer attachment, and rear wake can be identified as for the simple cubic case.

3. Figure 7, illustrating the profile through a side contact point at  $\alpha = 90$  deg. on the profile, is similar to the simple cubic packing profile illustrated in Figure 4. The point of contact is quite evident as a region, approximately 10 deg. wide, having essentially no mass transfer.

4. Figure 9 illustrates mass transfer rate profiles at a position of  $\beta = 54$  deg. 45 min. having contact points at  $\alpha = 60$  deg. and  $\alpha = 120$  deg. in addition to those at the top and bottom.

## CONCLUSIONS

The following conclusions can be drawn from the present work.

1. A method of fabricating benzoic acid test spheres having a diameter of 1.500 in. and of good quality and uniformity for mass transfer measurements was perfected. Also, a method for directly measuring the local radius around the spheres was perfected allowing determination of the local radius change with a probable error of  $\pm 0.00025$  in. This corresponds to a minimum probable percentage error of 0.8% for the maximum radius change of 0.0300 in. to 5% for a radius change of 0.0050 in.

2. A large variation in local mass transfer rates over the surface of a sphere in a packed bed exists. The maximum mass transfer rate was found to be up to three times

the average rate for simple cubic packing in a particle Reynolds number range of 488 to 2,409 and up to 3.8 times the average rate for rhombohedral packing in a particle Reynolds number range of 1,810 to 3,410.

3. Mass transfer rates in regions adjacent to points of contact between spheres are nearly zero for spheres in both simple cubic packing and rhombohedral packing. The size of these regions of minimum mass transfer rates depends on the location with respect to the flow direction. These regions covered a surface included in a solid angle of 20 deg. at the forward and rear points of contact which were hidden from the fluid flow, but were only 10 deg. across for points on the side of the spheres.

## ACKNOWLEDGMENT

The research of this paper was supported by Oak Ridge National Laboratory, AEC W7405 eng 26 Subcontract 2140. This support is gratefully acknowledged by the authors.

## NOTATION

$D_m$	= molecular diffusivity ( $D_v \rho_w / M_w$ ) g.-mole/cm.-sec.
$D_p$	= sphere diameter, 3.78 cm.
$D_v$	= volumetric diffusivity, sq. cm./sec.
$j_D$	= Colburn factor for mass transfer, $N_{Sh} / (N_{Re} N_{Sc}^{1/3})$
$j_H$	= Colburn factor for heat transfer, $N_{Nu} / (N_{Re} N_{Pr}^{1/3})$
$k_s$	= mass transfer coefficient, moles/sq. cm.-sec.-mole fraction
$M$	= molecular weight
$N_A$	= mass flux, moles/sq. cm.-sec.
$N_{Re}$	= particle Reynolds number ( $D_p V \rho_w / \mu_w$ ), dimensionless
$N_{Sc}$	= Schmidt number ( $\mu_w / \rho_w D_v$ ), dimensionless
$N_{Sh}$	= Sherwood number ( $k_s D_p M_w / \rho_w D_v$ ), dimensionless
$r$	= radius of test sphere, cm.
$T$	= temperature, °C.
$t$	= time, sec.
$\bar{V}$	= superficial velocity in test column, cm./sec.
$X$	= mole fraction

## Greek Letters

$\alpha$	= position angle on sphere from front stagnation point
$\beta$	= position angle on sphere from side contact point
$\rho$	= density, g./cu. cm.
$\mu$	= viscosity, cp.

## Subscripts

$BA$	= value of property for benzoic acid
$sat$	= value of property at saturation
$w$	= value of property for water

## LITERATURE CITED

- Baumeister, E. B., and C. O. Bennett, *A.I.Ch.E. Journal*, **4**, 69-74 (1958).
- Bird, R. B., W. E. Stewart, and E. N. Lightfoot, "Transport Phenomena," John Wiley & Sons, Inc., New York (1960).
- Garner, F. H., and J. M. Hoffman, *A.I.Ch.E. Journal*, **7**, 148-152 (1961).
- , and R. B. Keey, *Chem. Engr. Sci.*, **9**, 119-129 (1958).
- , and R. D. Suckling, *A.I.Ch.E. Journal*, **4**, 114-124 (1958).
- Glaser, M. B., and G. Thodos, *ibid.*, 63-68.
- Kramers, H., *Physica*, **12**, 61-80 (1946).
- Linton, W. H., and T. K. Sherwood, *Chem. Engr. Progr.*, **46**, 258-264 (1950).
- McAdams, W. H., "Heat Transmission," 3 ed., p. 265, McGraw-Hill, New York (1954).

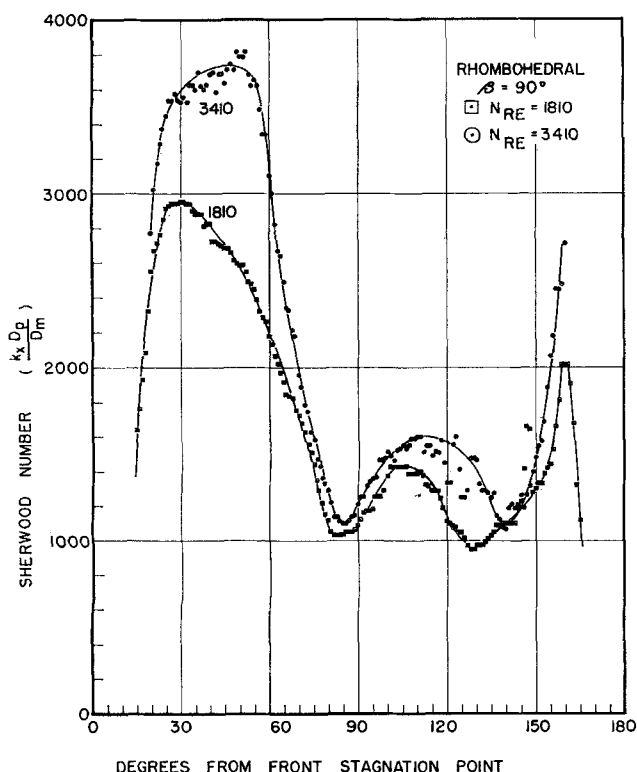


Fig. 10. Local Sherwood number profiles for spheres in rhombohedral packing. Profile position angle  $\beta = 90$  deg.

10. McCune, L. K., and R. H. Wilhelm, *Ind. Engr. Chem.*, **41**, 1124-1134 (1949).
11. Paul, T., *Z. Phys. Chem.*, **14**, 104-123 (1894).
12. Ranz, W. E., and W. E. Marshall, *Chem. Engr. Progr.*, **48**, 247-253 (1952).
13. Rhodes, J. M., M.S. thesis, Univ. Tennessee, Knoxville, Tennessee (1962).
14. Scarborough, J. B., "Numerical Mathematical Analysis," Johns Hopkins Press, Baltimore, Maryland (1958).
15. Seidell, A., "Solubilities of Organic Compounds," 3 ed., 2 vol., D. Van Nostrand, Princeton, N. J. (1941).
16. Sherwood, T. K., and R. L. Pigford, "Absorption and Extraction," McGraw-Hill, New York (1952).
17. Steele, L. R., and C. J. Geankopolis, *A.I.Ch.E. Journal*, **5**, 178-181 (1959).
18. Thoenes, D., Jr., and H. Kramers, *Chem. Engr. Sci.*, **8**, 271-283 (1958).
19. Treybal, R. E., "Mass Transfer Operations," McGraw-Hill, New York (1955).
20. Von der Decken, C. B., et al., *Chem.-Ing. Tech.*, **32**, 591-594 (1960).
21. Wadsworth, J., *Natl. Res. Council (Canada) Rept. MT-39*, (Sept. 12, 1958).
22. Ward, H. L., and S. S. Cooper, *J. Phys. Chem.*, **34**, 1484-1493 (1930).
23. Wilke, C. R., *A.I.Ch.E. Journal*, **1**, No. 2, 264-270 (1955).

*Manuscript received July 31, 1964; revision received December 11, 1964; paper accepted December 14, 1964. Paper presented at A.I.Ch.E. Chicago meeting.*

# Pressure Drop Studies in a Plate Heat Exchanger

VERNON C. SMITH and RALPH A. TROUPE

Northeastern University, Boston, Massachusetts

Recent studies on heat transfer in plate heat exchangers have pointed out the need for quantitative expressions for pressure drop in this type of apparatus. This paper presents the results of experimental studies to obtain pressure drop relationships useful in plate heater design.

A plastic prototype of a commercial model (Chester-Jensen) exchanger was fabricated and used to obtain entrance, exit, crossover, ribbed section, and overall pressure drops as a function of velocity with water as the fluid. These individual losses were combined into an expression for overall pressure drop for a series plastic plate pack having any number of plates and employing any fluid.

Overall pressure drop data on a commercial Chester-Jensen Model HTF plate heater were available from several heat transfer studies reported previously. The data for series patterns were resolved by inserting overall pressure drop, physical properties of the fluid, and number of plate passes into the general form of the equation derived for plastic plates and by solving for a new set of constants. The resulting computer-derived expression was found to predict series pressure drops in the apparatus to  $\pm 10\%$ .

From a similar approach it was possible to correlate the overall pressure drop data for the heater for looped flow patterns.

Although plate heat exchangers have been commercially available for many years (1, 2, 3), heat transfer and pressure drop data on these units have appeared in the literature only recently. Most of the available data deals only with heat transfer characteristics, with little attention given to pressure drop. This paper presents the results of the experimental pressure drop studies performed to develop data for plate heater design.

The heat transfer design of plate heaters is discussed by Buonopane (4) for turbulent flow in various plate arrangements of a Chester-Jensen model HTF exchanger. Jackson (5) has extended this work to the region of laminar flow in the same exchanger using corn syrup solutions.

In a typical plate heater the flow pattern is too complex for the theoretical derivation of velocity profiles and pressure drops. In these units the fluid enters and leaves a rec-